

### 13. Ultrasonic Measurement of Elastic Constants of Rocks under High Pressures\*.

By Hiroo KANAMORI and Hitoshi MIZUTANI,

Geophysical Institute, Faculty of Science,  
The University of Tokyo.

(Read Sept. 22, 1964.—Received Dec. 25, 1964.)

#### Abstract

Ultrasonic determinations of elastic constants of various rocks under high pressures up to 10 kilobars were made. The measurement includes both  $P$  and  $S$  wave velocity determinations. Accuracies in  $P$  and  $S$  wave velocity measurements are 1 and 2 per cent respectively. The variation of elastic constants as a function of pressure together with the data of the modal analysis is reported.

Discussions of the results are made with respect to the relation between  $P$  wave velocity  $V_P$  and density  $\rho$ , the effect of the serpentinization and also the Poisson's ratio of the various kinds of rocks.

A linear relation  $V_P=(2.8\rho-1.3)\pm 0.5$  km/sec is given. The partial serpentinization of 20 per cent reduces the  $P$  wave velocity of dunite to 7.5 km/sec and 50 per cent serpentinization reduces it to 6.8 km/sec. Although both eclogite and fresh dunite give about the same  $P$  wave velocity, eclogite gives a higher Poisson's ratio and density than dunite.  $P$  wave velocity, density and Poisson's ratio of fresh dunite are in the proximity of the values of the earth's upper mantle so far estimated from the seismological data. This is favourable to the peridotitic mantle hypothesis.

#### Introduction

The importance of determining the elastic constants of rocks under high pressures cannot be overemphasized for the interpretations of geophysical and seismological data.

Among the various methods which have so far been adopted, the ultrasonic method may give most reliable values of the elastic constants.

---

\* Communicated by T. Hagiwara.

In order to determine the elastic moduli such as compressibility and Poisson's ratio in isotropic substances, both  $P$  and  $S$  wave velocities should be determined on one and the same sample. Recently, Simmons<sup>1)</sup> determined  $S$  wave velocities under high pressures of various rock specimens of which Birch<sup>2)</sup> had previously determined the  $P$  wave velocities. Generally speaking, the ultrasonic determination of  $S$  wave velocities is more difficult than that of  $P$  wave velocities owing to the lack of proper transducers available for the measurement and also to the poor transmission of shear wave energy between a transducer and a specimen. As Simmons suggested in his paper it is necessary to increase the number of accurate  $S$  wave velocity determinations in order to make further comprehensive interpretations of the data so far accumulated by various geophysical and seismological observations.

In this connection, determinations of pressure dependence of elastic constants of various rock specimens by the ultrasonic pulse method were made in the present study. The measurement includes both  $P$  and  $S$  wave velocity determinations on one and the same specimen.

#### Method of Measurement

The technique adopted in this study is the ordinary pulse-echo method widely adopted by many investigators.

Accordingly, only a brief explanation of the method will be given in the following.

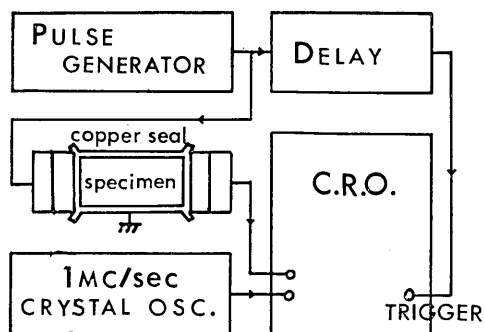


Fig. 1. Schematic diagram of equipment for measurement of velocity.

1) G. SIMMONS, "Velocity of Shear Waves in Rocks to 10 Kilobars, 1," *J. Geophys. Res.*, **69** (1964), 1123.

2) F. BIRCH, "The Velocity of Compressional Waves in Rocks to 10 Kilobars, 1," *J. Geophys. Res.*, **65** (1960), 1083.

Two lead zirconate transducers, either *P* or *S* type, are pressed at both ends of a specimen (Fig. 1). A transducer at one end is excited by an electrical pulse of 50 volt high and  $0.5\sim 3\ \mu$  sec wide, and the resulting ultrasonic pulse is started from this end. After being propagated lengthwise through the specimen it is converted again to an electrical pulse by the transducer at the other end. This pulse is amplified and displayed on an oscilloscope and the travel time is measured by either a 1 Mc/sec signal from a calibrated crystal oscillator or a mercury delay line. Knowing the travel time and the specimen length, the *P* or *S* wave velocities can be calculated.

In the following, several techniques which are particularly important for the measurement under high pressure and also for attaining an effective *S* wave generation and transmission between a transducer and a specimen will be noted.

#### *Sealing of Specimens*

Specimens are jacketed by a copper foil of 0.1 mm thick and by a pair of copper caps of 0.25 mm thick. The sealing method is similar to the one described by Hughes and Maurett.<sup>3)</sup> This method of sealing is the most perfect way of excluding the liquid pressure medium from the pores in rocks.

#### *Transducer*

The *P* wave transducer is a lead zirconate disk which is polarized normally to the disk surface. The natural frequency of the transducer commonly used in the measurement is 1 Mc/sec.

The *S* wave transducer is also a lead zirconate type. Four lead zirconate transducers of quadrantal shape, each transversally polarized, are pasted together in the shape of circular disk to form a *S* wave transducer. The natural frequency is 400 kc/sec. This transducer has a high electromechanical coupling factor compared with quartz crystal transducers.

It seems that the theory of the transmission of an ultrasonic pulse through a rod has not been thoroughly studied, and the effect of using transducers of different natural frequencies on wave velocities obtained therefrom has hitherto often been a subject of discussion.

As a preliminary test of the above we adopted transducers of various natural frequencies ranging from 200 kc/sec to 2 Mc/sec, and tested on aluminium and rhyolite specimens. The results are shown in Fig. 2.

3) D. S. HUGHES and C. MAURETTE, "Variation of Elastic Wave Velocities in Granites with Pressures and Temperature," *Geophysics*, **21** (1956), 277.

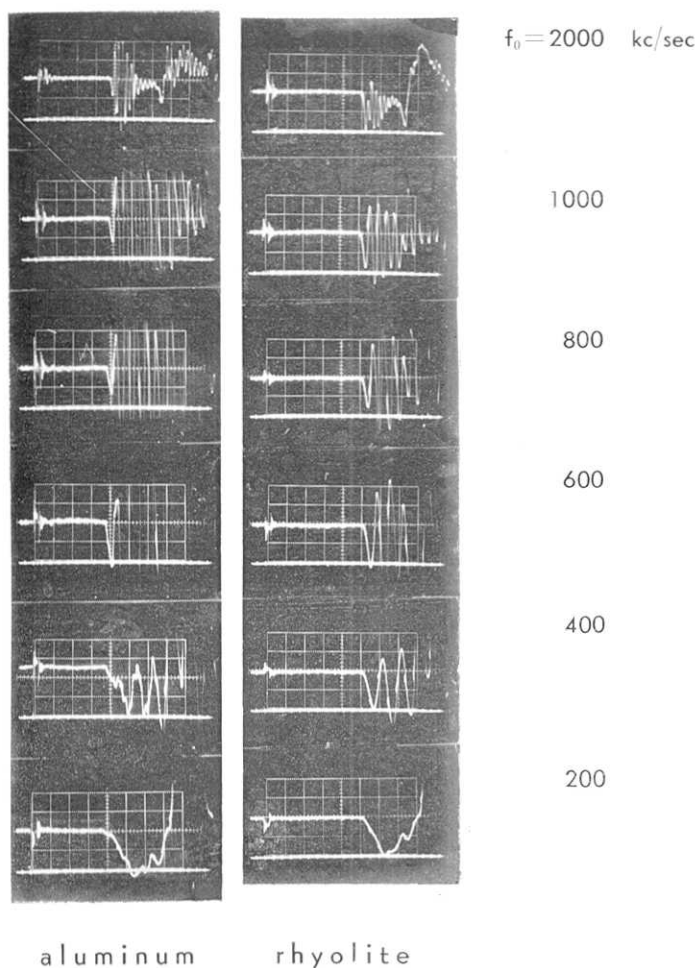


Fig. 2. Wave forms of acoustic pulses from transducers of various frequencies transmitted through aluminium and rhyolite specimens.

It is clear from this figure that so long as we read the onset time of the signal, no appreciable difference will result in the travel time reading.

#### *Coupling of Transducer*

In order to attain an effective transmission of the shear mode ultrasonic pulse, the transducers are tightly pressed to the specimen, with the copper cap in between, by a screw from a brass tubing which is slipped over the jacketed specimen. Although the copper caps have the effect

of reducing the transmission efficiency, acoustic energy sufficient enough to drive the pick-up transducer can be obtained when the lapping of the specimen surfaces and the sealing of specimens are carefully made.

#### Measurement of Time

Measurement of time was made either by a mercury delay line or a 1 Mc/sec timing signal from a quartz crystal oscillator. The measurement by a mercury delay line has the advantage of enabling a quick reading and of being less dependent on the observer. But the sharpness of the onset of the transmitted signal through the specimen more or less depends on both the specimen and confining pressure. The coarser the grain size and the lower the confining pressure, the more gradual the onset becomes. This makes the coincidence in shape between the signal from the specimen and that from the mercury delay line somewhat ambiguous. For this reason most of the data listed in Table 2 was obtained by using a calibrated 1 Mc/sec standard crystal oscillator.

The accuracy of the determination of the travel time depends mainly upon the sharpness of the onset of the transmitted signal. In the case

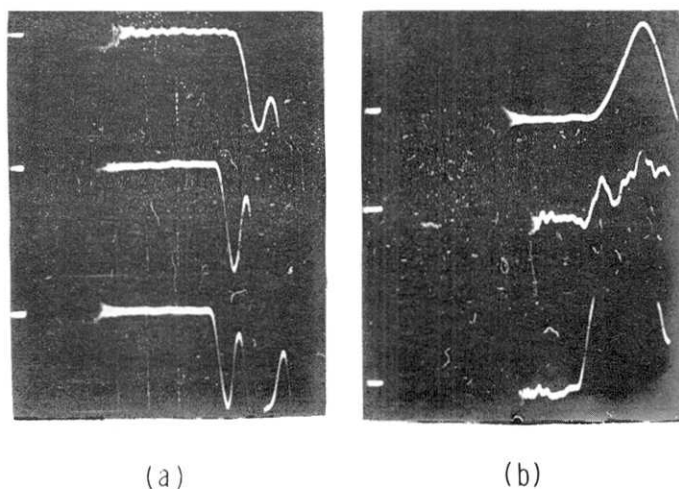


Fig. 3.

a) Received *P* wave signal.

The upper trace is the wave form at 1 atm. The trace in the middle is at 2 kb. The lower trace shows the sharp onset of the received signal at 10 kb. The vertical amplification is set at 1/10 of that used in ordinary measurements.

b) Received *S* wave signal.

Received *S* wave signals at 1 atm (top), 2 kb (middle), and 10 kb (lowermost).

Table 1. List of

Sample No.	Rock	Locality		
			olivine	pyroxene
0026	Dunite	Peridotite-gabbro complex Mikabu Zone, Miye Pref.	69	3
0028	Eclogite	Higashi-akaishi Peridotite mass, Ehime Pref.		42
0029	Peridotite	ditto	91	
0033	Dunite	Horoman Peridotite mass Hidaka, Hokkaido	88	2 (CPX**) 9 (OPX***)
0034	Plagioclase Peridotite	ditto	65	17
0035	Peridotite	ditto	79	5 (CPX) 14 (OPX)
0036	Serpentinized Peridotite	Higashi-akaishi Peridotite mass, Ehime Pref.	11	
0037	Peridotite	Peridotite-gabbro complex Mikabu zone, Miye Pref.	54	1 (CPX)
0038	Eclogite	Higashi-akaishi Peridotite mass, Ehime Pref.		42
0039	Plagioclase Peridotite	Peridotite-gabbro complex Mikabu zone, Miye Pref.	34	26 (CPX)
0041	Serpentinized Peridotite	Peridotite-gabbro complex Mikabu zone, Miye Pref.	45	1 (CPX)
0042	Diorite	Diorite in Ryoke Gneiss Dando area, Aichi Pref.		
0043	Serpentinized Peridotite	Waga, Iwate Pref.	41	
0045	Hornblende Gabbro	Ayabe, Kyoto		
0046	Peridotite	Peridotite-gabbro complex Mikabu zone, Miye Pref.	54	13
0048	Biotite Granodiorite	Senmaya area, Iwate Pref.		10 (CPX)
0049	Hornblende Granodiorite	Kuji, Iwate Pref.		
0050	Hornblende Granodiorite	Tejika, Iwate Pref.		
0051	Diopside- Hornblendite	Miyamori complex, Iwate Pref.		43
0052	Serpentinized Peridotite	ditto	33	
0053	Serpentinized Peridotite	ditto	43	

\* saussuritic aggregate after plagioclase (clinozoisite, albite etc.)

\*\* clino-pyroxene

\*\*\* ortho-pyroxene

the specimens

Modal Composition (Vol. %)						
serpentine + fine-grained magnetite	garnet	feldspar (plagio- clase)	quartz	hornblende	biotite + chlorite after biotite	rest
21		6*				1
	53			5		
9						0.5
		15				1
						3
						2
89						
40		3*				2
	53			5		
23		15*				2
51		3				
		41		46	14	
58						1
		31		68		1
24		7*				2
		74	10		6	
		57	19	8	16	
		69	15	5	10	
				57		
67						
57						

of *P* wave velocity determinations, the transmitted signal from the 1 Mc/sec transducer gives a signal on an oscilloscope sharp enough to obtain an accuracy better than 1 per cent. As shown in Fig. 3a, the onset becomes clearer when the confining pressure is raised. This increases the accuracy of the determination of time under high pressures. On the other hand, the *S* wave signal has a rather gradual onset under low pressures as shown in Fig. 3b. It can be noticed that no appreciable *P* wave energy is transmitted from this transducer. This is the advantage of using a *S* wave transducer of this type so that we can reduce the ambiguity involved in the identification of *S* phase. When the confining pressure is raised to about 2 kilobars, the *S* wave arrival is preceded by pulses originating from *P* waves as shown in Fig. 3b, and the identification of the onset of *S* phase becomes appreciably ambiguous. However, when the pressure is raised still further up to 10 kilobars, the transmission efficiency of the *S* wave gradually increases and the amplitude becomes very large compared with the forerunning *P* wave signals. As shown in the lowermost trace of Fig. 3b, the onset of *S* wave is clear enough at 10 kilobars to obtain a reading accuracy better than 2 per cent.

### High Pressure Apparatus

The whole assembly of the transducer and specimen is put in a high pressure cylinder having a piston from underneath. The inner and outer diameter of the cylinder is 30 mm and 220 mm respectively and the length is 300 mm. The upper cap of the cylinder has electrodes which are fixed and cemented by pyrophyllite and epoxy.

This cylinder is set on a 1000-ton Kennedy type press. The pressure medium is silicon oil of low viscosity. The pressure calibration was made by measuring the electrical resistance of a manganin coil put in the cylinder.

### Samples

All the samples used in this study were from numerous localities of Japan. Many of them are high density rocks such as dunite, peridotite and eclogite. To these are added some gabbroic rocks and granitic rocks. The list of the samples is given in Table 1. The modal composition was determined by Banno and Nakamura of the Geological Institute of Tokyo



Table 2. Variation of elastic constants as a function of pressure

P(kb)							
Sample		0	2	4	6	8	10
0026 $\rho=3.20 \text{ g/cm}^3$	$V_P(\text{km/sec})$	6.99	7.32	7.46	7.52	7.60	7.65
	$V_S(\text{km/sec})$	3.60	3.75	3.84	3.88	3.90	3.94
	$\sigma$	0.320	0.322	0.320	0.320	0.321	0.322
	$k(10^{10}\text{cgs})$	98	108	112	114	116	118
0028a $\rho=3.49$		7.64	8.14	8.30	8.38	8.45	8.48
		4.18	4.26	4.30	4.34	4.36	4.40
		0.287	0.312	0.318	0.317	0.317	0.317
		122	148	155	157	158	160
0028b $\rho=3.49$		7.54	8.10	8.18	8.30	8.38	8.40
		—	—	—	—	—	—
		—	—	—	—	—	—
		—	—	—	—	—	—
0029a $\rho=3.17$		7.14	7.38	7.60	7.70	7.80	7.84
		3.61	3.80	3.90	3.96	4.00	4.04
		0.328	0.320	0.321	0.320	0.322	0.319
		106	112	118	122	125	126
0029b $\rho=3.15$		6.98	7.22	7.35	7.42	7.46	7.48
		3.69	3.90	3.98	4.00	4.08	4.12
		0.305	0.294	0.294	0.292	0.289	0.284
		96	99	103	105	105	106
0029c $\rho=3.17$		6.66	7.00	7.22	7.35	7.44	7.46
		3.60	3.75	3.82	3.85	3.90	3.94
		0.293	0.298	0.303	0.309	0.310	0.308
		85	95	102	107	110	110
0033 $\rho=3.30$		7.71	8.16	8.36	8.45	8.50	8.52
		4.40	4.58	4.68	4.75	4.76	4.80
		0.256	0.271	0.270	0.267	0.267	0.267
		110	128	134	136	137	138
0034 $\rho=2.99$		7.11	7.58	7.70	7.78	7.85	7.90
		4.04	4.20	4.28	4.34	4.38	4.40
		0.260	0.275	0.271	0.274	0.281	0.281
		86	100	103	105	107	109

(to be continued)

Table 2-2.

(continued)

P(kb)		0	2	4	6	8	10
Sample							
0035 $\rho=3.30 \text{ g/cm}^3$	$V_P$	7.17	7.70	7.86	7.94	7.98	8.02
	$V_S$	4.00	4.14	4.16	4.18	4.20	4.22
	$\sigma$	0.272	0.298	0.306	0.309	0.311	0.311
	$k$	99	120	127	130	133	135
0036a $\rho=2.73$		5.64	5.80	5.90	6.02	6.10	6.16
		2.72	2.78	2.84	2.88	2.92	2.98
		0.348	0.348	0.350	0.350	0.349	0.347
		60	63	65	67	70	71
0036b $\rho=2.73$		6.03	6.18	6.28	6.35	6.42	6.50
		2.84	2.90	2.96	3.02	3.10	3.12
		0.357	0.357	0.356	0.353	0.351	0.350
		69	73	75	76	77	78
0037a $\rho=3.05$		6.44	6.64	6.76	6.84	6.88	6.92
		3.25	3.36	3.42	3.46	3.50	3.54
		0.329	0.325	0.323	0.324	0.324	0.323
		83	87	88	90	94	94
0037b $\rho=3.06$		6.34	6.52	6.65	6.76	6.80	6.88
		3.19	3.26	3.30	3.38	3.42	3.48
		0.332	0.335	0.335	0.334	0.332	0.329
		81	87	90	93	94	95
0037c $\rho=3.07$		6.44	6.60	6.70	6.78	6.84	6.90
		3.12	3.28	3.38	3.44	3.48	3.50
		0.346	0.333	0.329	0.328	0.326	0.326
		87	89	91	93	94	96
0038a $\rho=3.52$		7.14	8.25	8.44	8.54	8.58	8.60
		4.12	4.35	4.46	4.52	4.56	4.60
		0.249	0.305	0.306	0.305	0.303	0.301
		100	149	156	159	161	161
0038b $\rho=3.51$		6.98	8.12	8.28	8.35	8.40	8.45
		3.96	4.14	4.26	4.32	4.38	4.40
		0.260	0.324	0.320	0.315	0.313	0.312
		97	149	154	156	158	159

(to be continued)

Table 2-3. (continued)

Sample	$P(\text{kb})$	0	2	4	6	8	10
		$V_P$	6.84	7.92	8.20	8.32	8.38
0038c		—	—	—	4.46	4.53	4.56
$V_S$		—	—	—	0.296	0.292	0.294
$\rho=3.50 \text{ g/cm}^3$		—	—	—	149	150	152
0039		6.94	7.20	7.30	7.40	7.60	7.62
		3.70	3.86	3.94	4.00	4.02	4.05
$\rho=3.13$		0.302	0.298	0.296	0.292	0.288	0.283
		93	99	102	103	103	103
0041		6.50	6.60	6.65	6.74	6.80	6.88
		3.26	3.32	3.38	3.40	3.45	3.50
$\rho=3.04$		0.331	0.329	0.328	0.327	0.328	0.326
		85	87	88	90	92	94
0042a		6.30	6.52	6.66	6.78	6.82	6.84
		3.38	3.45	3.48	3.52	3.55	3.58
$\rho=2.94$		0.297	0.308	0.311	0.314	0.314	0.314
		71	79	82	85	86	87
0042b		6.58	6.68	6.75	6.80	6.85	7.00
		3.38	3.50	3.54	3.58	3.60	3.62
$\rho=2.93$		0.322	0.313	0.310	0.310	0.310	0.310
		82	83	84	85	87	87
0042c		6.70	6.85	6.94	6.98	7.00	7.02
		3.38	3.50	3.54	3.58	3.60	3.62
$\rho=2.96$		0.328	0.324	0.324	0.326	0.321	0.322
		87	90	92	93	93	94
0043b		6.77	7.00	7.15	7.20	7.22	7.22
		3.64	3.72	3.80	3.86	3.95	4.00
$\rho=2.82$		0.297	0.302	0.303	0.297	0.287	0.279
		79	85	90	89	88	86
0043c		6.54	6.78	6.92	7.00	7.05	7.10
		3.54	3.60	3.62	3.64	3.68	3.70
$\rho=2.82$		0.293	0.304	0.309	0.312	0.314	0.314
		73	81	84	87	90	90

(to be continued)

Table 2-4.

(continued)

Sample	$P(\text{kb})$	0	2	4	6	8	10
		$V_P$	6.60	6.96	7.02	7.06	7.10
0045a $\rho=3.11 \text{ g/cm}^3$	$V_S$	3.54	3.65	3.75	3.78	3.82	3.85
	$\sigma$	0.297	0.302	0.304	0.298	0.295	0.295
	$k$	82	95	96	95	95	95
0046a $\rho=3.14$		6.87	7.02	7.15	7.20	7.26	7.30
		3.58	3.68	3.72	3.78	3.80	3.82
		0.314	0.312	0.314	0.315	0.313	0.313
		94	98	102	104	105	105
0046b $\rho=3.15$		6.67	6.90	7.02	7.12	7.18	7.22
		3.58	3.68	3.72	3.78	3.80	3.82
		0.298	0.300	0.304	0.305	0.303	0.305
		86	92	97	99	101	101
0048 $\rho=2.69$		5.95	6.18	6.28	6.36	6.40	6.45
		3.30	3.45	3.56	3.64	3.68	3.70
		0.276	0.268	0.266	0.260	0.253	0.255
		55	59	61	61	61	61
0049 $\rho=2.71$		5.72	6.12	6.26	6.34	6.40	6.48
		3.18	3.45	3.54	3.56	3.58	3.60
		0.275	0.264	0.263	0.265	0.268	0.273
		52	58	60	62	64	65
0050 $\rho=2.77$		4.56	6.18	6.46	6.54	6.60	6.65
		2.80	3.18	3.30	3.35	3.38	3.45
		0.199	0.314	0.323	0.322	0.322	0.322
		28	66	74	76	78	79
0051 $\rho=3.20$		5.75	6.92	7.08	7.16	7.20	7.25
		3.44	3.75	3.90	3.96	4.00	4.02
		0.220	0.293	0.281	0.275	0.278	0.280
		55	93	95	96	98	100
0052 $\rho=2.85$		6.40	6.64	6.70	6.78	6.80	6.82
		3.43	3.55	3.65	3.70	3.72	3.74
		0.299	0.292	0.290	0.290	0.290	0.290
		72	76	77	79	80	80
0053 $\rho=2.92$		6.11	6.38	6.55	6.64	6.72	6.75
		3.22	3.26	3.30	3.34	3.38	3.42
		0.308	0.322	0.329	0.329	0.329	0.329
		68	77	82	84	86	88

University.

This determination was made by Leitz integration stage and by taking the average of about 15 cm scanning.

The specimens of rock were first cored and ground to the right circular cylinder of 22 mm in diameter and 30~70 mm long.

When the specimen is large enough two or three cylinders are cut in mutually perpendicular directions.

### Numerical Data

The results of the measurements are given in Table 2. The values of  $P$  wave velocity  $V_P$  and  $S$  wave velocity  $V_S$  were directly calculated from the travel time measurement, and Poisson's ratio  $\sigma$  and incompressibility (bulk modulus)  $k$  were calculated therefrom. In this table are added the values of the density measured by the Archimedes principle.

Three examples are also shown in Figs. 4, 5 and 6. In Fig. 4, as an

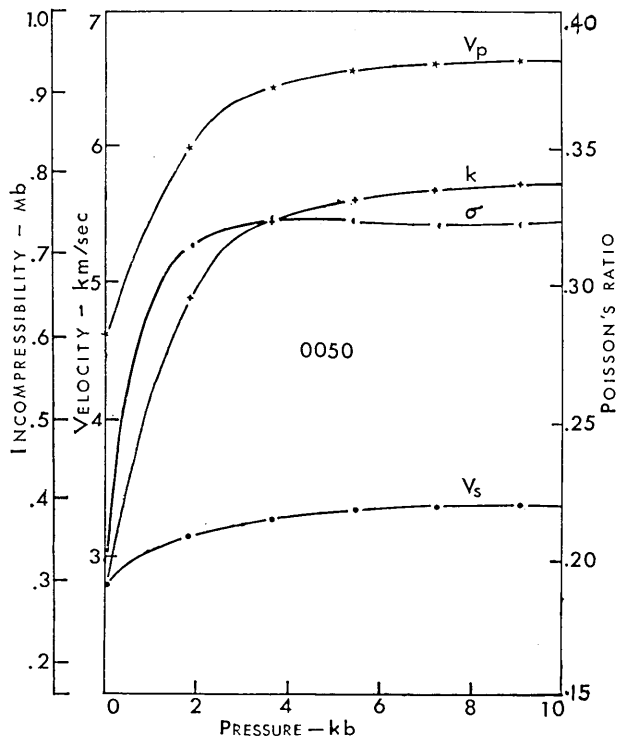


Fig. 4. The variation of elastic constants with pressure for granodiorite.

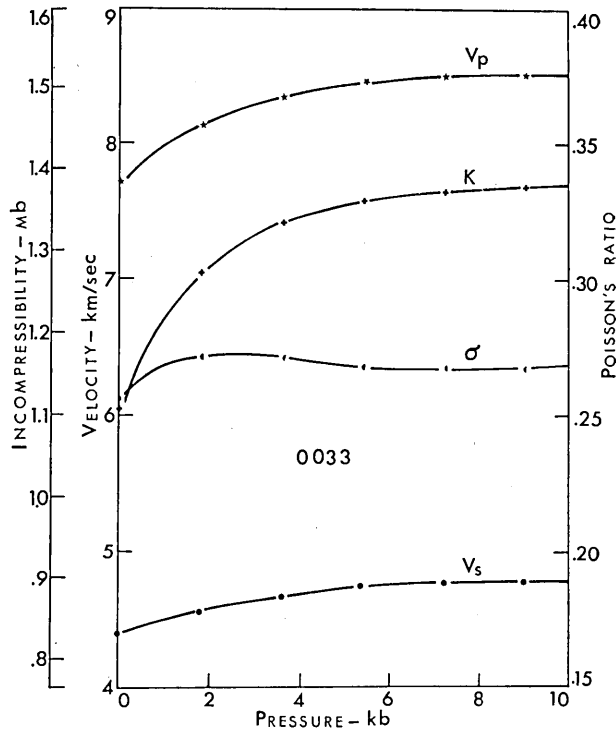


Fig. 5. The variation of elastic constants with pressure for dunite.

example of a granitic rock, the variation with pressure of various elastic constants of granodiorite is shown.

The remarkable increase in  $V_p$  with the increase in pressure up to 2 kilobars indicates the rapid decrease of the porosity. It should be noted that Poisson's ratio also rapidly increases with pressure which implies that the  $P$  wave velocity increases more rapidly than  $S$  wave velocity, in other words,  $P$  wave velocity is more sensitive to the porosity than  $S$  wave velocity.

As an example of dunite, we took a specimen No. 0033. This is a fresh dunite from Horoman and completely free from serpentinization. The  $P$  and  $S$  wave velocities are about 8.5 km/sec and 4.8 km/sec respectively at 10 kilobars. This dunite consists mainly of olivine (88%) as shown in Table 1.

The eclogite specimen gives more rapid increase in wave velocity with pressure than the dunite (Fig. 6). The velocity value is about 8.5 km/sec over the pressure range from 4 kilobars to 10 kilobars.

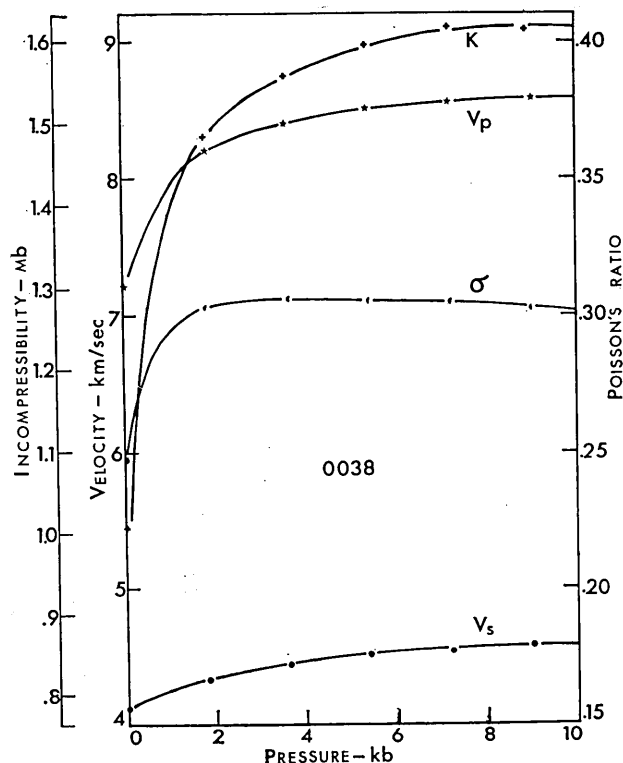


Fig. 6. The variation of elastic constants with pressure for eclogite.

From these three examples and also from other data listed in Table 2, it may be said that the Poisson's ratio does not vary appreciably after the pore space in rocks is reduced by the confining pressure. For the rocks of comparatively high porosity such as specimen No. 0050 and 0038 illustrated above, the Poisson's ratio increases very sharply with the pressure variation up to 2 kilobars. On the contrary, for the rocks of low porosity, such as specimen No. 0033, the change of the Poisson's ratio with pressure is very gradual.

This is consistent with the direct conclusion from Murnaghan's theory of finite strain that the pressure has only a second order effect on the Poisson's ratio.

### Discussion of Results

#### Velocity

Although the velocity value under high pressures may be free from

the effects of porosity and textures, it strongly depends on the mineralogical composition of the individual rock.

As an example of this, the wave velocity of dunite and peridotite depends mainly upon the amount of serpentine and pyroxene contained. The strongest controlling factor of the density and velocity of peridotite is the serpentinization. This is clearly seen in Table 2 with the values of velocity and density of the specimens No. 0026, 0037, 0041, 0052, 0053 etc. which are partly serpentinized. This problem will be treated in the later discussion but it should be noted here that the serpentinization as slight as 10 per cent can reduce the values of velocity and density to values appreciably less than 8 km/sec and 3.2 g/cm<sup>3</sup> respectively. These values are significantly lower than the average values for the upper mantle of the earth.

Next to the serpentinization, the pyroxene content in peridotite has also some effects on the wave velocity. A typical dunite No. 0033 shown in Fig. 5 consists mainly of olivine (90%) and pyroxene (10%) and has the *P* wave velocity of about 8.5 km/sec at 10 kilobars. On the other hand, the amount of olivine in the specimen No. 0035 which is from the same locality as that of No. 0033 is reduced from 90 per cent to 80 per cent, increasing the pyroxene content to 20 per cent. The associated *P* wave velocity change is from 8.5 to 8.0 km/sec at 10 kilobars. The increasing fractional content of pyroxene may further decrease the *P* wave velocity of peridotite.

From these considerations it may be concluded that if dunite is the main constituent rock of the upper mantle it should have more than 80 per cent olivine to give the *P* wave velocity around 8.1 km/sec, which is the average mantle velocity estimated from the seismological observations. The ratio of olivine to pyroxene of 8:2 to 9:1 may be most probable for the peridotitic mantle.

Although eclogite (0038) and dunite (0033) give approximately the same *P* wave velocity, the density of eclogite is higher than dunite. The normal mantle density of the earth has been estimated at 3.3 g/cm<sup>3</sup> by various geophysical implications, and the values obtained here with dunite are in the proximity of this value. On the contrary, the density 3.5 g/cm<sup>3</sup> for eclogite appears too high. For this reason, as Clark and Ringwood<sup>4)</sup> suggested, the possibility of eclogite being the main constituent rock of the upper mantle might be rejected.

4) S. P. CLARK Jr. and A. E. RINGWOOD, "Density Distribution and Constitution of the Mantle," *Rev. Geophys.*, 2 (1964), 35.



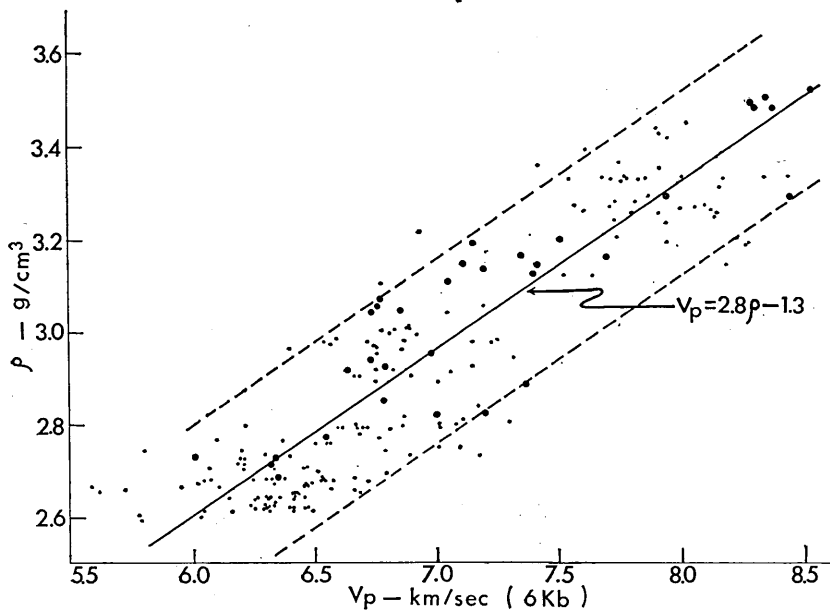


Fig. 7.  $P$  wave velocity at 6 kb versus density. Large circles indicate the values obtained in the present study and small circles are from the data by Birch.

#### *Relation between velocity and density*

The relation between wave velocity and density has been discussed by Woollard<sup>5)</sup> and Birch.<sup>6)</sup> Birch gives an approximately linear relationship between  $V_p$  and  $\rho$  with the mean atomic weight as a parameter.

In Fig. 7, we plotted our data together with the data obtained by Birch. In this figure, while the positive correlation is clearly seen, the individual measurement appreciably scatters, so that no single curve of the form  $V_p = a\rho + b$  can be fitted. One possible method is to fit the data by a group of straight lines having the mean atomic weight as a parameter, as Birch did. However, for the purpose of studying crustal structures it is often required to estimate the density values from the known velocity values or vice versa without knowing the mean atomic weight. For this reason, a simple convenient relation is given here al-

5) G. P. WOOLLARD, "Crustal Structure from Gravity and Seismic Measurements," *J. Geophys. Res.*, **64** (1959), 1521.

6) F. BIRCH, "The Velocity of Compressional Waves in Rocks to 10 Kilobars, 2," *J. Geophys. Res.*, **66** (1961), 2199.

lowing for the scattering of the data, which is

$$V_P = (2.8\rho - 1.3) \pm 0.5 \text{ km/sec} \quad (\rho \text{ in g/cm}^3).$$

This relation is shown by a solid line in Fig. 7. The dashed lines in this figure show the possible range of the variation previously used by Kanamori<sup>7)</sup> for the study of crustal structure in Japan.

#### *Serpentinization*

As is well known, the serpentinization of dunite decreases both density and velocity. Although the gross composition might also have some effects, the serpentine content may most strongly affect the values of density and velocity. From Table 2, we took the values of *P* wave velocity at 10 kilobars and density for peridotites, and plotted them against the individual serpentine content by volume per cent. The result

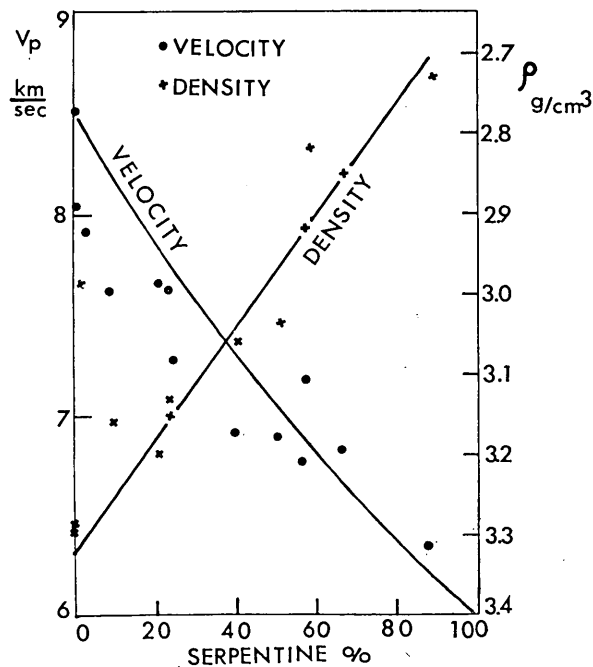


Fig. 8. Effect of serpentinization on velocity and density of peridotite. (at 10 kilobars)

Solid curves show the theoretical relations for ideal serpentine-olivine aggregates.

7) H. KANAMORI, "Study on the Crust-mantle Structure in Japan, 2," *Bull. Earthq. Res. Inst.*, **41** (1963), 761.

is shown in Fig. 8. In this figure are added the theoretical curves for ideal serpentine-olivine aggregates given by Birch.<sup>8)</sup> Although the density curve approximates the data well, the velocity curve gives, for a fixed serpentine content, velocity values about 0.2 km/sec larger than the values we obtained. This may be due to the effects of other constituent minerals in our specimens such as pyroxenes and plagioclase.

In any case, the serpentinization of the order of 20% can reduce the velocity of dunite to 7.5 km/sec and that of about 50% can reduce it to 6.8 km/sec. The low  $P$  wave velocity in the upper part of the upper mantle of some places, notably Japan (Aki,<sup>9)</sup> Kaminuma and Aki,<sup>10)</sup> Kanamori,<sup>11)</sup>) has often been discussed. If this reduction in the wave velocity in the upper mantle is due solely to the partial serpentinization of the dunite of the mantle, the required value of the degree of the serpentinization is about 10~20%. This value is not unlikely.

#### *Poisson's ratio*

The controlling factor of the Poisson's ratio is still very difficult to understand. Molotova and Vassilév<sup>12)</sup> have tabulated the Poisson's ratio so far determined by various methods, either by field observations or by laboratory experiments. However, no systematic relation of Poisson's ratio to chemical composition and other elastic constants can be seen.

In the present study, we have calculated the Poisson's ratio from measured  $V_P$  and  $V_S$  values, but in order to obtain accurate values of Poisson's ratio, a great accuracy in both  $P$  and  $S$  wave determinations is required. As is easily shown,

$$|\Delta\sigma/\sigma| \leq 3\{|\Delta V_P/V_P| + |\Delta V_S/V_S|\}.$$

In the present study,  $|\Delta V_P/V_P| = 0.01$ ,  $|\Delta V_S/V_S| = 0.02$  and resulting uncertainty in  $|\Delta\sigma/\sigma|$ , in the most pessimistic case, would be about 10 per cent.

With this understanding we plotted the Poisson's ratio against the  $P$  wave velocity at 10 kilobars (Fig. 9). The specimens are classified

8) F. BIRCH, *loc. cit.*, 6).

9) K. AKI, "Crustal Structure in Japan from the Phase Velocity of Rayleigh Waves, 1," *Bull. Earthq. Res. Inst.*, **39** (1961), 255.

10) K. KAMINUMA and K. AKI, "Crustal Structure in Japan from the Phase Velocity of Rayleigh Waves, 2," *Bull. Earthq. Res. Inst.*, **41** (1963), 243.

11) H. KANAMORI, "Study on the Crust-mantle Structure in Japan, 3," *Bull. Earthq. Res. Inst.*, **41** (1963), 801.

12) L. V. MOLOTOVA and YU. I. VASSIL'EV, "Velocity Ratio of Longitudinal and Transverse Waves in Rocks, 1, 2," *Bull. Acad. Sci. USSR, Geophys. Ser.* (1960), 930. 1097.

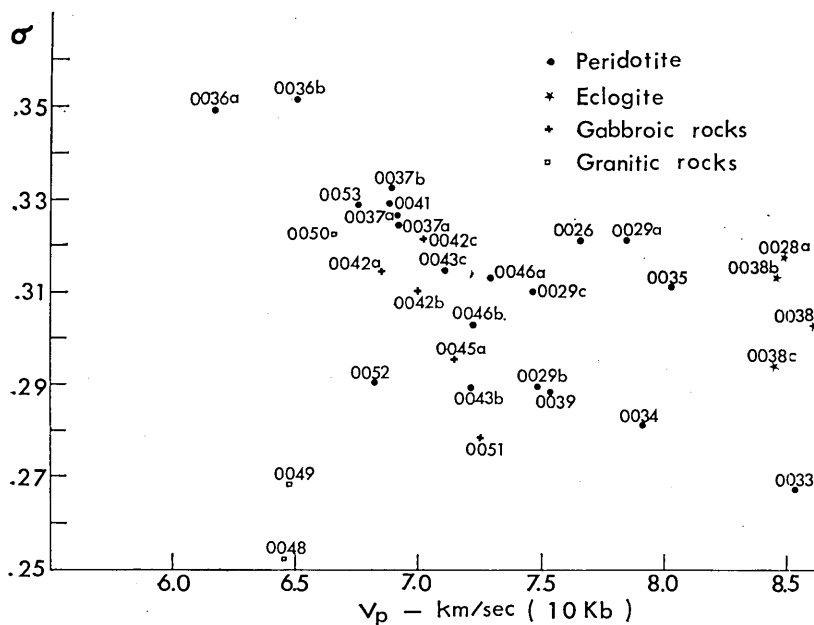


Fig. 9. Poisson's ratio at 10 kilobars versus  $P$  wave velocity at 10 kilobars.

into four groups, 1st group consists of peridotitic rocks; 2nd, eclogite; 3rd, gabbroic rocks and 4th, granitic rocks. From this figure, it can be concluded that eclogite has the Poisson's ratio of around 0.31 and gabbroic rocks have the values around 0.30. With the exception of the specimen No. 0050, granitic rocks have rather small Poisson's ratio of about 0.26. Inspection of this figure leaves the impression that there may be a negative correlation between  $V_p$  and  $\sigma$  of peridotitic rocks. A typical dunite 0033 has the largest value of  $V_p$  but the smallest value of  $\sigma$  ( $=0.27$ ). When the velocity is reduced with the increasing fractional content of minerals other than olivine, mainly of serpentine, the Poisson's ratio increases up to 0.35.

From the seismological data so far obtained, the Poisson's ratio of the upper mantle should be about 0.27. It should not exceed 0.30 at the largest. As is mentioned above, the Poisson's ratio of eclogite, though the data is scanty, is about 0.31 and only a fresh dunite which has more than 80 per cent of olivine has Poisson's ratio of about 0.27. It could be said that a peridotitic mantle, which consists mainly of dunite having olivines of more than 80 per cent in volume is more com-

patible with the present result than the eclogitic mantle.

More accurate determination of the Poisson's ratio is desirable to clarify a systematic dependence of the Poisson's ratio of rocks on the chemical composition.

### Acknowledgment

We are indebted to Prof. H. Kuno of the Geological Institute of Tokyo University, who kindly provided us with all the rock specimens used in this study. We are also grateful to Dr. S. Banno and Mr. Y. Nakamura of the Geological Institute of Tokyo University for their kindness in giving us the data of the modal analysis of the specimens. Drs. S. Akimoto and S. Minomura of the Institute for Solid State Physics, Tokyo University, afforded us every facility for using high pressure apparatus of the Institute which is gratefully acknowledged.

### 13. 高圧下における岩石の弾性定数の測定

東京大学理学部 { 金 森 博 雄  
地球物理学教室 { 水 谷 仁

10 kb までのいろいろな岩石の弾性定数を測定した。測定法はジルコン酸鉛のトランスデューサーを用いて、 $P$ ,  $S$  の弾性波を発生し、その走時より  $V_P$ ,  $V_S$  を求めるものである。サンプルは直径 22 mm, 長さ 30~70 mm の円柱状に成型し、空隙内に圧力媒体の油が浸み込むことを防止するため、薄い銅板でシールした。走時の測定には主に 1 Mc/sec の水晶発振器を用いた。圧力装置には 1000 トンのケネディ型プレスを用いた。トランスデューサーの固有振動数は縦波の場合 1 Mc/sec, 横波の場合 400 kc/sec である。トランスデューサーの固有振動数が弾性波の速度に及ぼす影響はいろいろ論じられてきたが、Fig. 2 にみるように、200 kc/sec から 2 Mc/sec に至る各種のトランスデューサーを用いても、走時のよみとりには大きな差はみられない。

サンプルは日本各地からのもので、Table 1 にモード分析の結果を合わせて示してある。大部分は dunite, peridotite, eclogite のような密度の大きな岩石である。

$V_P$ ,  $V_S$  が独立に測定されたので、これらよりポアソン比  $\sigma$  と非圧縮率  $k$  を計算した。これらの弾性定数の圧力変化の例が Fig. 4, Fig. 5, Fig. 6 に図示されている。全てのサンプルについての結果が Table 2 に掲げてある。2 kb までに  $V_P$  が著しく増加することは porosity の急激な減少によるものであることを示す。ポアソン比の同様な変化を考え合わせると、 $V_P$  は  $V_S$  よりも porosity の影響を強く受けることがわかる。ポアソン比は空隙がなくなると、圧力変化をうけないようにみえる。これは Murnaghan の有限歪の理論から予想されることと矛盾しない。得られた測定結果をもとにして次のことが議論される。

#### 1) 速 度

高圧下での速度は岩石の鉱物組成に依存している。例えば peridotite, dunite の速度は主に serpentine, pyroxene の含量に依存している。特に serpentinization は peridotite の密度や速度の大きな支配因子である。10% の serpentinization をうけた peridotite の  $V_P$  は 8 km/sec 以下、密度は 3.2 g/cm<sup>3</sup> 以下になる。pyroxene の量も  $V_P$  に影響を与える。90% の olivine と 10

% の pyroxene からなる dunite の速度は 8.5 km/sec であるのに対し, 80% の olivine, 20% の pyroxene からなる dunite の速度は 8.0 km/sec になる. 地震波よりみつめられる値と合わせるためには, 上部マントルの構成物を dunite とすれば, その鉱物組成は olivine: pyroxene = 8:2, または 9:1 であると結論される.

速度はまた密度と正の相関をもつ. Fig. 7 に Birch の実験結果と共に,  $V_P$  対  $\rho$  の関係をプロットしてある. この関係から

$$V_P = (2.8\rho - 1.3) \pm 0.5 \text{ km/sec}$$

なる簡単な関係式を導くことができる.

## 2) Serpentinization

dunite 中の serpentine の量が増すと, 密度と速度が減少する. この関係を Fig. 8 に示してある. これから Birch によつて与えられた理論曲線が, 密度に関してよく成り立ち, 速度に関しては, われわれの実験値よりも約 0.2 km/sec 大きな値を与えることがわかる. これは, serpentine, olivine 以外の鉱物による影響と思われる.

いくつかの地域の上部マントルの上層に  $V_P$  の遅い層があることが論じられてきているが, もしこれを地域的な serpentinization の結果であるとする, 必要な serpentinization の値は 10~20% 程度である.

## 3) ポアソン比

ポアソン比を支配する因子を理解することは難しいし, われわれの測定もポアソン比については最悪の場合 10% 程度の誤差がある. われわれの結果についてポアソン比と  $V_P$  の関係をプロットすると Fig. 9 のようになる. この関係から eclogite は  $\sigma=0.31$ , gabbroic rocks は  $\sigma=0.30$ , granitic rocks は  $\sigma=0.26$  で,  $V_P$  と無相関にみえるが, peridotitic rocks については  $\sigma$  と  $V_P$  が負の相関をもっているようである. 地震波から推定される上部マントルのポアソン比は約 0.27 であるから, 80% 以上の olivine を含む dunite のみがこの条件に適する. このことおよび速度と密度の値から考えて, 上部マントルの構成物としては, eclogite よりも olivine を 80% 程度含む dunite を考えるのが都合がよい. しかし, 上にも述べたように Poisson 比の測定にはかなりの誤差があると思われるので, このことについて決定的な結論を下すためにはさらに測定の精度を上げ, 数を増やす必要がある.